S. KASTELIC, J. MEDVED, P. MRVAR

ISSN 0543-5846
METABK 49(4) 301-305 (2010)
UDC – UDK 669.05:621.791.052:608.4=111

PREDICTION OF NUMERICAL DISTORTION AFTER WELDING WITH VARIOUS WELDING SEQUENCES AND CLAMPINGS

Received – Prispjelo: 2009-11-23
Accepted – Prihvaćeno: 2010-01-15
Original Scientific Paper – Izvorni znanstveni rad

Welding simulation of a test cover for hydropower plant was made due to very large dimensions of the cover. The main aim was to predict distortion after welding in order to avoid machining the cover. Welding process was simulated with the Sysweld program to keep distortion in desired limits. Various welding sequences and clamping conditions were calculated to reduce the distortion. Calculation of microstructure constituents in virtual complex geometry of joints was also analyzed.

Key words: welding simulation, finite element method, multipass welding, distortion prediction

Numeričko predviđanje izobličenja nakon zavarivanja s različnim slijedom zavarivanja i spajanja. Simulacija zavarivanja testnog pokrova hidroelektrane provedena je zbog velikih dimenzija ispitne prevlake. Osnovni je cilj predvidjeti izobličenje nakon zavarivanja. Radi postizanja veličine izobličenja u željenim granicama proces zavarivanja je simuliran programom Sysweld. Različiti tijekovi zavarivanja i uvjeta spajanja proračunati su radi smanjenja izobličenja. Određivanje mikrostrukturnih konstituenata u virtualnoj komleksnoj geometriji spojeva je također provedeno.

Ključne riječi: simulacija zavarivanja, metoda konačnih elemenata, zavarivanje u više slojeva, predviđanje izobličenja

INTRODUCTION

Welding is an important process and has significant role in industry, especially in automotive, marine and energy industries.

Knowledge of all the properties and welding parameters enables prediction of final distortion. Accurate prediction of distortion is important when distortion of some unique, big parts has to be predicted. In order to keep deformation in desirable limits, changes of welding parameters, such as welding sequence and clamping of the welded parts, may be needed. If change of welding parameters for a complex part, with big number of beads or multipass welding is made, then it is not easy to predict distortion after the welding [1, 2].

In order to obtain all the needed data with numerical calculation, all the main physical effects that accrue in welding must be taken in account. All results were calculated with the modified heat convection equation (1). It enables to perform non-linear computations with all the material properties that depend on temperature, phase and material transformations, fractions of chemical elements and other accompanying variables [3-5].

Numerical simulation was used to predict final distortion after welding a test cover for hydro-power plant. Test cover is shown in Figure 1. Its diameter is 5,5 m and flange on the cover is 120 mm thick. Making the cover is not issue of this paper. Cover was welded and then machined in workshop to desirable dimensions. Problem occurred with transport. These test cover will be used in a reversible hydro-power plant that is located high in the Alps – about 2000 m above the sea level. Transport of 5,5 m diameter test cover by road is not possible because tunnels are not big enough. Transport with helicopter is also not possible because the cover is too heavy at 2000 m above the sea level. So test cover must be cut to two halves for transport by road and then welded together at the hydro-power plant place.

$$\left(\sum_i P_i(\rho C)_i\right)\frac{\partial T}{\partial t} - \nabla\left(\left(\sum_i P_i\lambda\right)\nabla T\right) + \sum_{i<j} L_{ij}(T)A_{ij} = Q \qquad (1)$$

$\boldsymbol{P}$ phase proportion
$\boldsymbol{T}$ temperature
$\boldsymbol{t}$ time
i, j phases
ρ mass density
$\boldsymbol{C}$ specific heat
λ thermal conductivity
$\boldsymbol{Q}$ heat sources
$\boldsymbol{L_{ij}(T)}$ latent heat of $i \rightarrow j$ transformation
$\boldsymbol{A_{ij}}$ proportion of phase i transformed to j in time unit

The goal of this numerical simulation was to predict distortion after welding and to determine welding sequences to keep distortion in tolerances. Thus welding

S. Kastelic, J. Medved, P. Mrvar, Faculty of Natural sciences and engineering, University of Ljubljana, Ljubljana, Slovenia

Figure 1 CAD model of test cover

will be performed without machining after the welding process.

PREPARING FEM MESH FOR CALCULATIONS

Finite elements mesh of test cover with Visual Mesh program was prepared for this calculation. The finite elements mesh for calculation is shown in Figure 2. Only half of the test cover was meshed because symmetry was taken into account.

Two simulations with different welding sequences and clamping conditions were made. The sequence for the first simulation started with welding on the flange. First 17 beads were made from the top of flange and continued with second 17 beads from the lower side of flange. Then 26 beads were made on the upper side of flange and at the end the rest of 26 beads on the lower side of flange. Together there were 86 beads altogether on flange. After flange was welded on the cover, welding of cover itself started, at first with six beads on the top and then with six beads on the lower side of cover. Welding sequence on flange is presented in Figure 3. In calculation with the first sequence, the clamping was minimal, it was without reinforcement plates, as shown in Figure 2. These plates were taken into account in the second calculation.

In the second simulation, also welding sequence was changed. Welding started on the upper side of cover

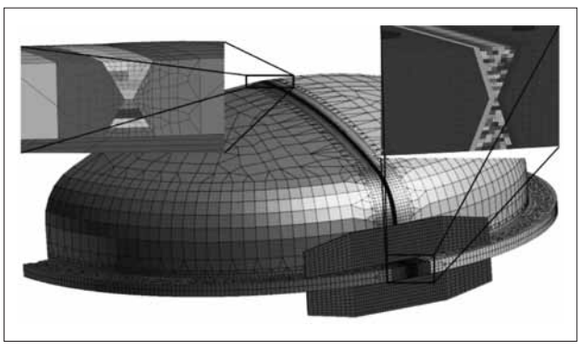

Figure 2 FEM mesh of the test cover

Figure 3 Welding sequence on flange

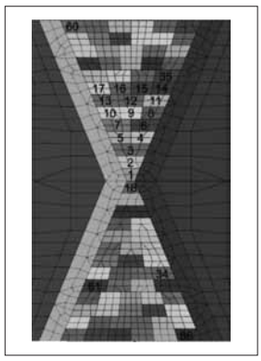

Table 1 **Welding parameters**

	Flange	Cover
Electrode	EVB 50	EVB 50
Current type	DC / +	DC / +
Electrode size	3,25 / 4 / 5	3,25 / 4
Current	110-130 / 140-160 / 180-200 A	110-130 / 140-150 A
Voltage	24-26 / 25-27 / 26-28 V	24-26 / 25-27 V
Welding speed	15-20 / 20-25 / 25-30 cm/min	12-15 / 15-18 cm/min

with 6 beads and continued with 17 beds on the upper side of flange. Afterwards, 6 beads were welded onto the lower side of cover and welding continued with 17 beads on the lower side of flange. Then welding continued on the upper side of flange with 26 beads and finished with 26 beads on lower side of flange. Clamping was also changed. In the second simulation, the clamping was stiffer and reinforcement plates, as shown in Figure 2, were included into the calculation.

DEFINING HEAT INPUT

Defining the heat input is based on actual welding parameters that are presented in Table 1. These parameters are also important for preparation of mesh. Volume of deposited material for each bead is determined with electrode size and welding speed. Energy input is defined with welding current, voltage and welding speed.

Defined heat input is based on the size of test cover and on welding parameters. The method, applied in this particular case, is called "Macro weld deposit methodology". Heat is transferred into weld instantaneously in one or several macro steps. Real weld trajectory is divided into several macro sections. It was included into the structure before the beginning of computation and omitted after definition of the macro time steps. Energy/length ratio that is transferred into the structure is the same as in actual process, but it is taking place in another time frame.

Heat input for each bead on flange was defined in one single macro step. Temperature distribution during the cooling after the last bead has been welded onto flange is presented in Figure 4.

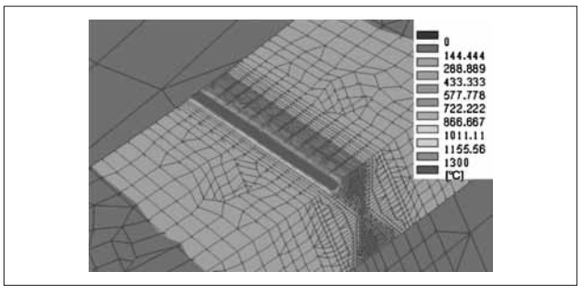

Figure 4 Temperature distribution after welding the last bead on flange

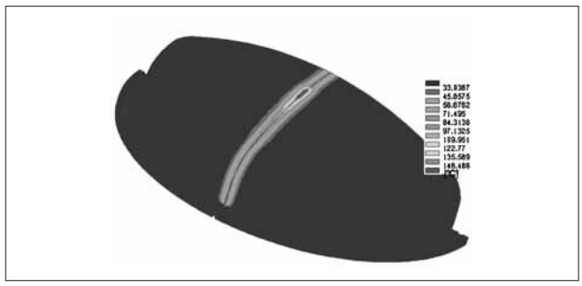

Figure 5 Temperature distribution during the first bead on cover

Table 2 **Chemical composition of St355 steel**

Element	C	Si	Mn	P	S	Al	N	Cr	Cu	Ni
Composition in wt%	0,18	0,47	1,24	0,029	0,029	0,024	0,0085	0,10	0,17	0,06

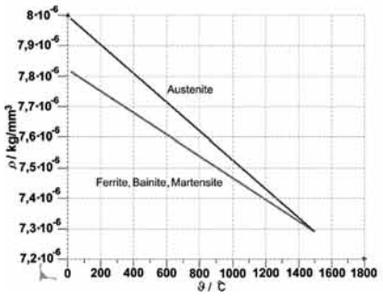

Figure 6a Density

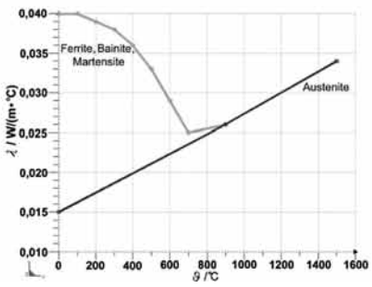

Figure 6b Thermal conductivity

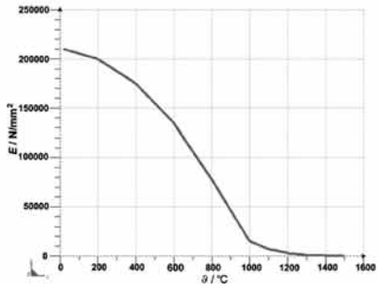

Figure 6c Young's modulus

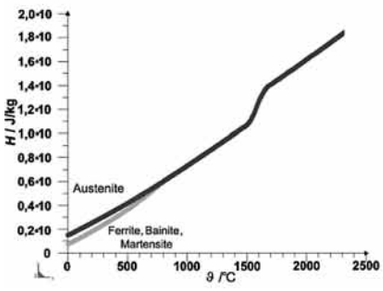

Figure 6d Latent heat

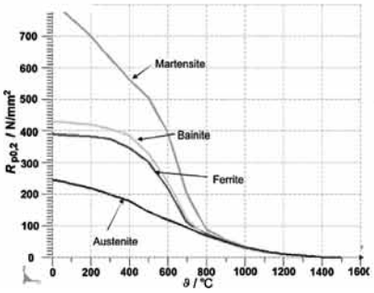

Figure 6e Yield stress

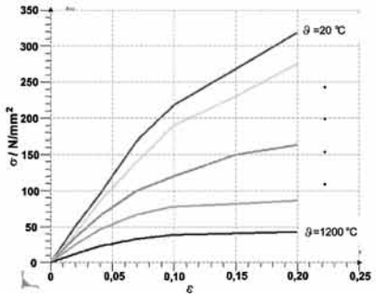

Figure 6f Strain hardening

Heat input on the cover was defined for each bead with ten macro steps. It meant that weld on the cover was divided into ten segments.

Heat was then defined for each segment separately with time delay between single segments. Time delay between segments depended on the length of segment and on the welding speed. Temperature distribution during welding the first bead onto the cover is shown in Figure 5.

DEFININING MECHANICAL PROPERTIES

Base material of the cover is St355 steel with chemical composition presented in Table 2. In order to obtain reliable numerical results, precise thermal and material properties of the used material must be taken in account. All these properties must be measured as functions of temperature and phases. Yield stress, thermal strains, Young's modulus, Poisson ratio, strain hardening, density, thermal conductivity and latent heat must be known for quality welding. Some of these properties are presented in graphs in Figures 6a to 6f.

Digitalized CCT diagram is needed for calculation of microstructural constituents. Diagram is presented in Figure 7.

RESULTS

With all these data several results for deformation after welding can be obtained. In our case, deformation after welding was the main goal. Next to deformation,

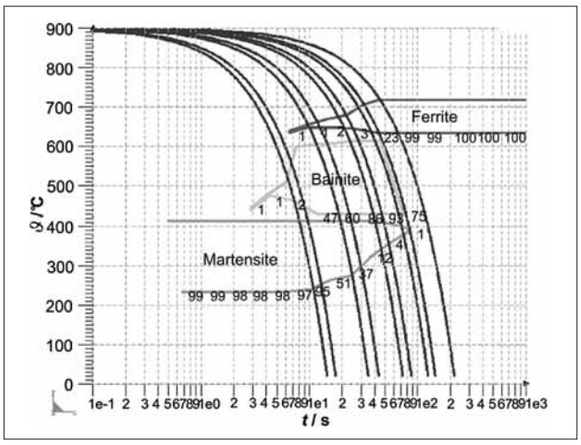

Figure 7 CCT diagram of St355 steel

very important parameters are also stresses and microstructure in the welding area after the welding.

Deformation of test cover after the welding with the second sequence in the flange area was less than 2 mm. The deformed shape of the cover is presented in Figure 8. In this picture wireframe of cover before welding and also the deformed shape afterwards are presented. The deformed shape was multiplied by 20 so that deformed shape is more pronounced.

Effect of various welding sequences and clamping conditions is presented in Figures 9a and 9b. Maximum deformation after welding with the first sequence was 4,3 mm. Deformation of test cover on the X-axis after welding is shown in Figure 9a.

Welding with the second sequence resulted in smaller deformation. The deformation on the X-axis, shown in Figure 9b, is smaller and it is less than 2 mm. The deformed shape in Figures 8 and 9 is multiplied by 20.

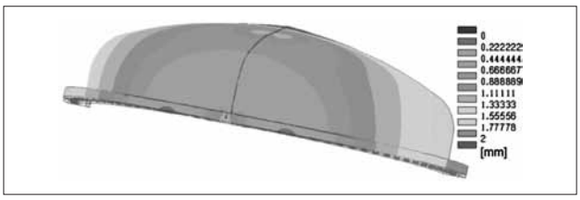

Figure 8 Deformation after welding with the first sequence

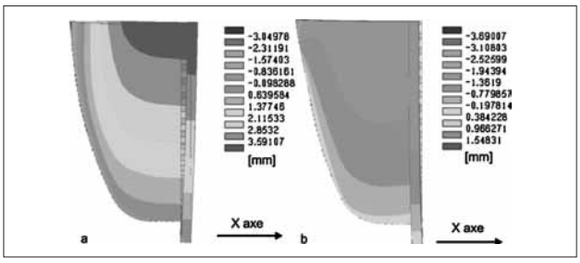

Figure 9 Deformation in the X-axis after welding, a) first sequence, b) second sequence

Next to deformation also distribution of stresses in heat affected zone was calculated. It became obvious that there was compressive stress in the middle of flange where first beads were weld onto flange, Figures 10a and 10b. The highest tensile stress was found under the surface of flange and in the area where last beads were welded.

The results that are presented in Figures 11a, 11b, 12a, and 12b show the microstructure of the heat affected zone after welding. Figures 11a and 11b present distribution of bainite in the welding area. The amount of bainite in the beads was quite high (90 vol. %) since preheating of area was 150 °C. Increased amount of martensitic phase, being between 10 to 20 vol. %, was found on the interface between base material and

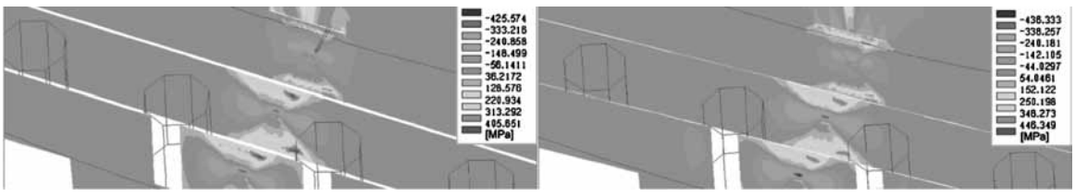

Figure 10 Stresses after welding with first sequence (a), and second sequence (b)

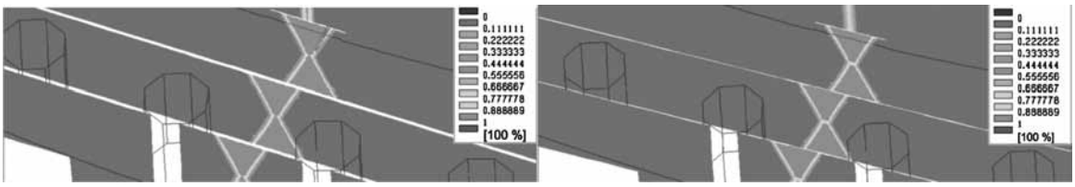

Figure 11 Bainite distribution after welding with first sequence (a), and second sequence (b)

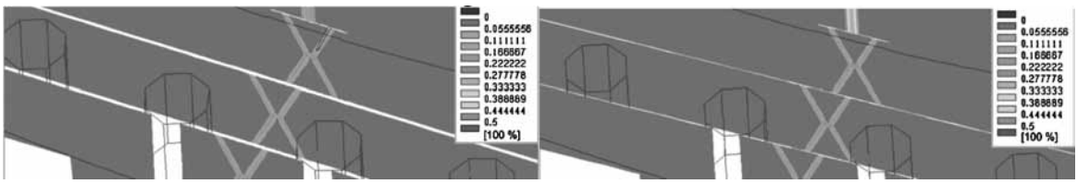

Figure 12 Martensite distribution after welding with first sequence (a), and second sequence (b)

welded-on beads. This was result of higher cooling rates at the interface with the base material. Distribution of martensite is presented in Figures 12a and 12b.

CONCLUSION

In order to predict distortion after welding the cover, two simulations were made with various welding sequences and clamping conditions. Deformation with the second simulation was smaller. In order to reduce deformation further, another calculation with changed welding sequence could be made, but obtained results were satisfactory for now. Peak values of stresses were relatively high for this material, but these peaks referred to very small areas. Also these values should be moderated with some simple trial welding under similar conditions. Trial welding should be simulated too that a comparison could be made whether these stresses would cause some cracks or not. Absolute values of stresses in the second case were slightly higher since clamping in the second case was more rigid, because the reinforcement plates were taken into consideration.

Amount of martensitic phase on the interface could be reduced with higher preheating temperature, but higher temperature could be hardly reached because heat capacity of cover was big. Also the possibility of cracks was relatively small because the areas with higher fraction of martensite did not appear on the same spots as the areas with high stresses.

REFERENCES

[1] D. Deng, H. Murakawa, W. Liang: Comput. Methods Appl. Mech. Engrg., 196 (2007), 4613–4627

[2] T. Schenk, I. M. Richardson, M. Kraska, S. Ohnimus: Computational Materials Science, 45 (2009), 999–1005

[3] ESI Group: Sysweld reference manual, digital version SYSWELD 2008.1

[4] F. Boitout, D. Dry, P. Mourgue, H. Porzner, Y. Gooroochurn: Transient Simulation of Welding Processes - Thermal, Metallurgical and Structural Model, Sysweld v2004

[5] F. Boitout, D. Dry, P. Mourgue, H. Porzner, Y. Gooroochurn: Distortion control for large maritime and automotive structures, Sysweld v2004

Note: The responsible person for English language is prof. dr. A. Paulin.